ADVANCED MATERIALS
www.advmat.de

Strain Engineering of 2D Materials: Issues and Opportunities at the Interface

Zhaohe Dai, Luqi Liu, and Zhong Zhang**

Triggered by the growing needs of developing semiconductor devices at ever-decreasing scales, strain engineering of 2D materials has recently seen a surge of interest. The goal of this principle is to exploit mechanical strain to tune the electronic and photonic performance of 2D materials and to ultimately achieve high-performance 2D-material-based devices. Although strain engineering has been well studied for traditional semiconductor materials and is now routinely used in their manufacturing, recent experiments on strain engineering of 2D materials have shown new opportunities for fundamental physics and exciting applications, along with new challenges, due to the atomic nature of 2D materials. Here, recent advances in the application of mechanical strain into 2D materials are reviewed. These developments are categorized by the deformation modes of the 2D material–substrate system: in-plane mode and out-of-plane mode. Recent state-of-the-art characterization of the interface mechanics for these 2D material–substrate systems is also summarized. These advances highlight how the strain or strain-coupled applications of 2D materials rely on the interfacial properties, essentially shear and adhesion, and finally offer direct guidelines for deterministic design of mechanical strains into 2D materials for ultrathin semiconductor applications.

1. Introduction

2D materials are a relatively new class of atomically thin materials with emerging properties that lend well to next-generation ultrathin semiconductor devices.[1,2] Mechanical strain can strongly perturb the band structure of these materials, giving rise to the possibility of using mechanical deformation to tune their electronic and photonic performance dramatically.[3] In fact, this principle, termed strain engineering, is now routinely used in manufacturing traditional semiconductor devices.[4] The strain engineering of 2D materials is particularly exciting because an individual atomic sheet is intrinsically capable of sustaining much larger mechanical strain compared to either their bulk counterparts or conventional electronic materials.[5,6] Also, the thinness of 2D materials allows one to induce large local strains by poking, bending, or folding the material like a piece of paper.[7] These exceptional circumstances create opportunities for the study of new fundamental physics and applications of 2D materials emerging at large strain levels.[8–10] Considering difficulties associated with building a microelectromechanical system for straining freestanding 2D materials,[11] 2D materials were often transferred onto a substrate such that the strain can be introduced to the 2D material by controlling the deformation of the bulk substrate.[12] Such fact has led to significant advances in the strategies for straining 2D materials with a film-substrate system, as well as in interface metrologies for the van der Waals (vdW) interaction between the 2D material and its substrate.

Here, we first summarize recent experimental achievements on realizing mechanical strain to substrate-supported 2D materials by categorizing the deformation modes of the 2D material–substrate system. These deformation modes include in-plane modes caused by epitaxy, thermal-expansion mismatch, and stretching/compressing the substrate, as well as out-of-plane modes caused by wrinkling and buckling of 2D materials, bulging and poking 2D materials, and transferring 2D materials on a patterned substrate. We then review recent experimental characterizations of the mechanical response of 2D material–substrate interfaces to in-plane shear deformations and out-of-plane delamination. This is not meant to be an all-encompassing analysis of the broad-field topic of strain engineering, but instead, we point out how mechanical deformations are achieved into 2D materials within the film/substrate system and how the mechanics of interfaces govern these deformation mechanisms. The goal is to deterministically apply both strain magnitude and strain distribution into these atomically thin films and ultimately achieve strain-coupled fundamental physics and chemistry, and exciting applications in a controllable manner. Considering the interdisciplinary nature of research in this field, we also refer the readers to comprehensive reviews from relevant perspectives, including synthesis of emerging 2D materials, characterizations of the strain in 2D materials (especially via the Raman spectroscopy), and applications of mechanically strained 2D materials.[6,13,14]

2. In-Plane Mode

Strain engineering of traditional semiconductors has been leveraged to reduce intervalley scattering, increase mobility

Z. Dai, Prof. L. Liu, Prof. Z. Zhang
CAS Key Laboratory of Nanosystem and Hierarchical Fabrication
CAS Center for Excellence in Nanoscience
National Center for Nanoscience and Technology
Beijing 100190, P. R. China
E-mail: liulq@nanoctr.cn; zhong.zhang@nanoctr.cn

DOI: 10.1002/adma.201805417

in Si transistors, and reduce the hole effective mass in III–V semiconductor lasers.[15] Growth on epitaxial substrates with a controlled lattice constant mismatch has been widely utilized to establish in-plane strain.[16] This method can extend to the strain-engineered growth of atomically thin 2D materials (**Figure 1**a).[12,17] Some reports have demonstrated apparent strain in chemical vapor deposition (CVD) grown 2D materials.[18] Theoretical studies have also suggested that for 2D Mo and W-dichalcogenide monolayers, the in-plane epitaxial strain might be utilized to transform them from the semiconducting phase to a stable metallic phase.[19] In addition, epitaxial growth of 2D transition-metal dichalcogenide (TMD) heterojunctions, including vertical and lateral, introduces a new strain engineering strategy to produce novel electronic structures.[2,20–23] Note that the lattice-match strain can also be introduced by mechanically subjecting the 2D material to a periodic potential, e.g., transferring graphene on top of hexagonal boron nitride (hBN). In this case, both commensurate and incommensurate states were observed, depending on the rotation angle between the lattices of the two 2D materials, which can considerably alter the electronic and optical properties of the heterostructure.[24,25]

Thermal strain represents another type of residual strain in CVD-grown 2D materials, which is caused by the thermal-expansion mismatch between the 2D material and its substrate.[16,26] Both compressive and tensile strain can be achieved in the 2D material by selecting a substrate with different thermal properties (Figure 1b). Recently, Ahn et al. demonstrated stable built-in strains ranging from 1% tension to 0.2% compression by growing WSe_2 (9.5 ppm) on substrates with different thermal coefficient of expansion ranging from 0.55 to 12 ppm.[17] Notably, besides the growth method, postheating/cooling of the 2D material–substrate system can offer a controllable way to apply thermal strain.[27,28] In this context, the substrate is not limited to crystalline, and complex strain patterns in the 2D material can be achieved by applying nonuniform heat profiles in a designed fashion on such substrates.[27]

The most straightforward way to achieve in-plane strain in 2D materials may come from transferring them on a flexible substrate and directly stretching, compressing, or bending the substrate (Figure 1c).[29–37] This strategy allows simultaneous applications of mechanical strain and measurements of Raman and photoluminescence (PL) responses of the 2D material. By this, recent studies have demonstrated continuous tuning of the electronic structure of monolayer and multilayer TMDs using in-plane strain.[31] Alternatively, after the Raman and PL response of many 2D materials to strain are calibrated, their monolayered nature makes them of particular promise for wireless strain-sensor applications as demonstrated in Figure 1c.[35]

3. Out-of-Plane Mode

Due to their atomic thinness, 2D materials energetically favor out-of-plane deformations when subjected to a mechanical field. The out-of-plane configuration is typically an indicator of the release of the global in-plane deformations, limiting the accumulation of strain by the above-discussed in-plane loading mode. However, the considerable local strain and strain gradient associated with them have recently been utilized in the development of the strain engineering of 2D materials. In the following, we focus on strain engineering of 2D materials by wrinkles and buckles, bubbles and tents, and conformable patterns. The readers are referred to comprehensive reviews on out-of-plane deformation modes including ripples, folds,

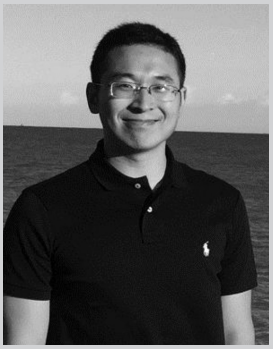

Zhaohe Dai worked as a joint graduate student at the National Center of Nanoscience and Technology, China from 2012 to 2016. He received his B.S. in modern mechanics from the University of Science and Technology of China in 2013 and his M.S. in solid mechanics from the Institute of Mechanics, Chinese Academy of Sciences in 2016. He is currently pursuing his Ph.D. at the University of Texas at Austin. His research interests are in the mechanics of 2D materials and their interfaces.

Luqi Liu is currently a professor at the National Center of Nanoscience and Technology, China. She received her Ph.D. from the Institute of Chemistry at the Chinese Academy of Sciences in 2003. After that, she undertook postdoctoral research in the Department of Materials and Interfaces at the Weizmann Institute of Science (Israel). In March 2007, she joined NCNST. Her current research focuses on the mechanics of nanomaterials as well as polymer-based nanocomposites.

Zhong Zhang is a full professor and the head of division at the National Center for Nanoscience and Technology, China. He obtained his bachelor, master, and Ph.D. degrees from the University of Science and Technology of China in 1990, 1996, and 1999, respectively. In 2001, he was granted the Sofja Kovalevskaja Award by the Alexander von Humboldt Foundation, which supported him to establish an independent research group at the Institute for Composite Materials, University of Kaiserslautern, Germany. He was recruited by NCNST in 2005. His major research interests are multifunctional polymer nanocomposites, nanomechanics, nanostructured surfaces and coatings, nanomanufacturing, and their applications.

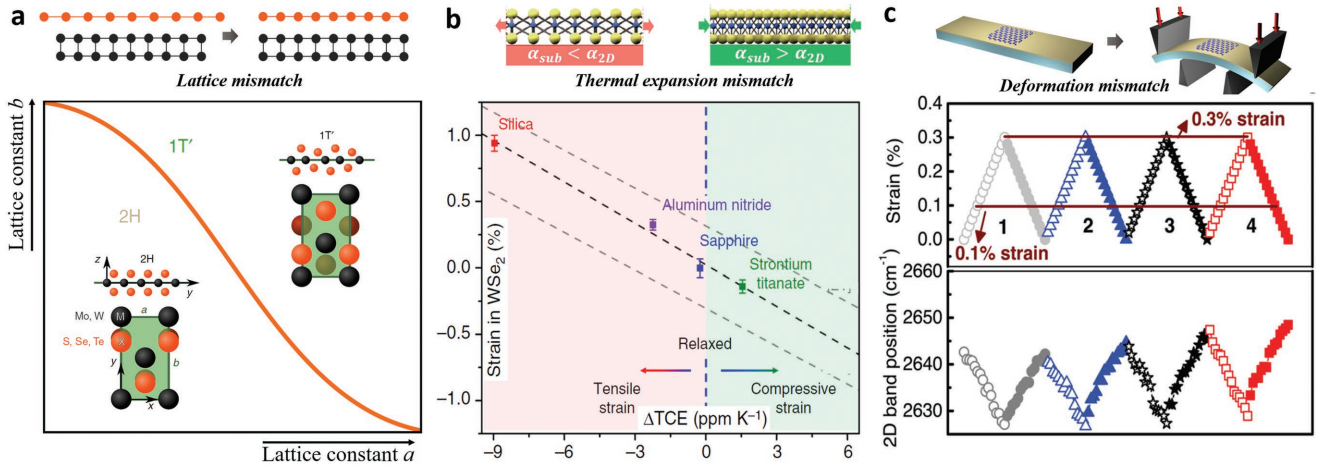

Figure 1. In-plane mode. a) Strain caused by lattice mismatch. For a TMD monolayer, its lattice parameters *a* and *b* by the growth substrate (shown in blue) can be used to select a particular phase of the TMD monolayer. Reproduced with permission.[19] Copyright 2014, Nature Publishing Group. b) Strain caused by thermal-expansion mismatch. Both compressive/tensile strain can be achieved in 2D materials based on the mismatch of thermal coefficient of expansion (ΔTCE) between the substrate and a monolayer WSe_2. Reproduced with permission.[17] Copyright 2017, Nature Publishing Group. c) Top panel: Scheme of straining the 2D material by deforming its supporting substrate. Reproduced with permission.[29] Copyright 2009, American Physical Society. Bottom panel: The sequence of the deformation and the response of 2D band position of an exfoliated graphene. Reproduced with permission.[35] Copyright 2014, Wiley-VCH.

scrolls, crumples for interesting functionalities of 2D materials such as surfaces with controllable wettability and transparency and flexible electronics.[38,39]

3.1. Wrinkles and Buckles

When a 2D material is under in-plane compression, it often leads to the formation of surface wrinkles or buckle delamination as a result of buckling instability.[40–43] As illustrated in **Figure 2**a–c, compressive strain to 2D materials can be introduced by directly compressing/prestretching the substrate, applying thermal stress, and growing/transferring 2D materials on the substrate (including 2D materials themselves) with a relatively smaller lattice constant. On a relatively stiff substrate, buckle delamination is typically observed (Figure 2d–f).[32,44–47] On a relatively compliant substrate, wrinkles are more likely to occur (Figure 2g–i).[22,43,45,48,49] In some systems, wrinkles and buckle-delamination blisters can co-exist and co-evolve by controlling the magnitude of the applied compressive strain.[41,50] Of particular interest is the localized strain at the crest of these buckles and wrinkles, where the curvature reaches the maximum. Recent studies have shown that such localized strain can alter the electronic and optical properties of 2D materials remarkably, such as reduction of the direct band gap in MoS_2 multilayers and up to 0.7 eV shift of the absorption edge in black phosphorus flakes.[46,49]

3.2. Bubbles and Tents

Many applications of 2D materials involve multiple transfer processes of 2D materials to a substrate, by which 2D material blisters, such as bubbles and tents, frequently form by trapping water, gas, or solid nanoparticles at the interface (**Figure 3**).[51–54] Initially, these circular blisters have been viewed as an inconvenience for device applications.[55,56] However, recent studies have shown considerable in-plane strain associated with these out-of-plane bubbles and tents, which creates opportunities for the study of new fundamental physics and applications of 2D materials emerging at large strain level.[10,57–59] Alternatively, many 2D material bubbles and tents are designedly created by confining interface liquid[51,60] and prepatterning substrates (Figure 3b),[59,61,62] respectively. Famous examples include the highly strained bubble-like and tent-like graphene,[10] which have been shown to possess large pseudo-magnetic fields, up to 300 *T* (Figure 3c), as well as 2D semiconductors draping over an array of micropillars, which can be applied as large-scale quantum emitters (Figure 3d).[59]

3.3. Conformable Patterns

Due to the high flexibility of 2D materials and their vdW interaction to the substrate, out-of-plane deformed 2D materials can be directly achieved by transferring them onto patterned substrates (**Figure 4**).[62–64] This method has led to significant development of the design of substrate patterns, along with strategies to fully conform 2D materials to them.[64–68] The resulting configurations have been recently exploited in many situations, where the associated mechanical strains in the 2D materials couple with interface chemistry and physics. For example, Nemes-Incze et al. used atomic force microscope (AFM) tips to indent a SiO_2-supported graphene flake such that the substrate underwent plastic deformation, and the graphene flake was still pinned to the deformed substrate.[67] This procedure can readily "write" out-of-plane profiles as demonstrated by the line- and dot-shaped graphene in Figure 4a. Zheng and co-workers transferred MoS_2 to SiO_2 nanocones using capillary pressure (Figure 4b) and demonstrated

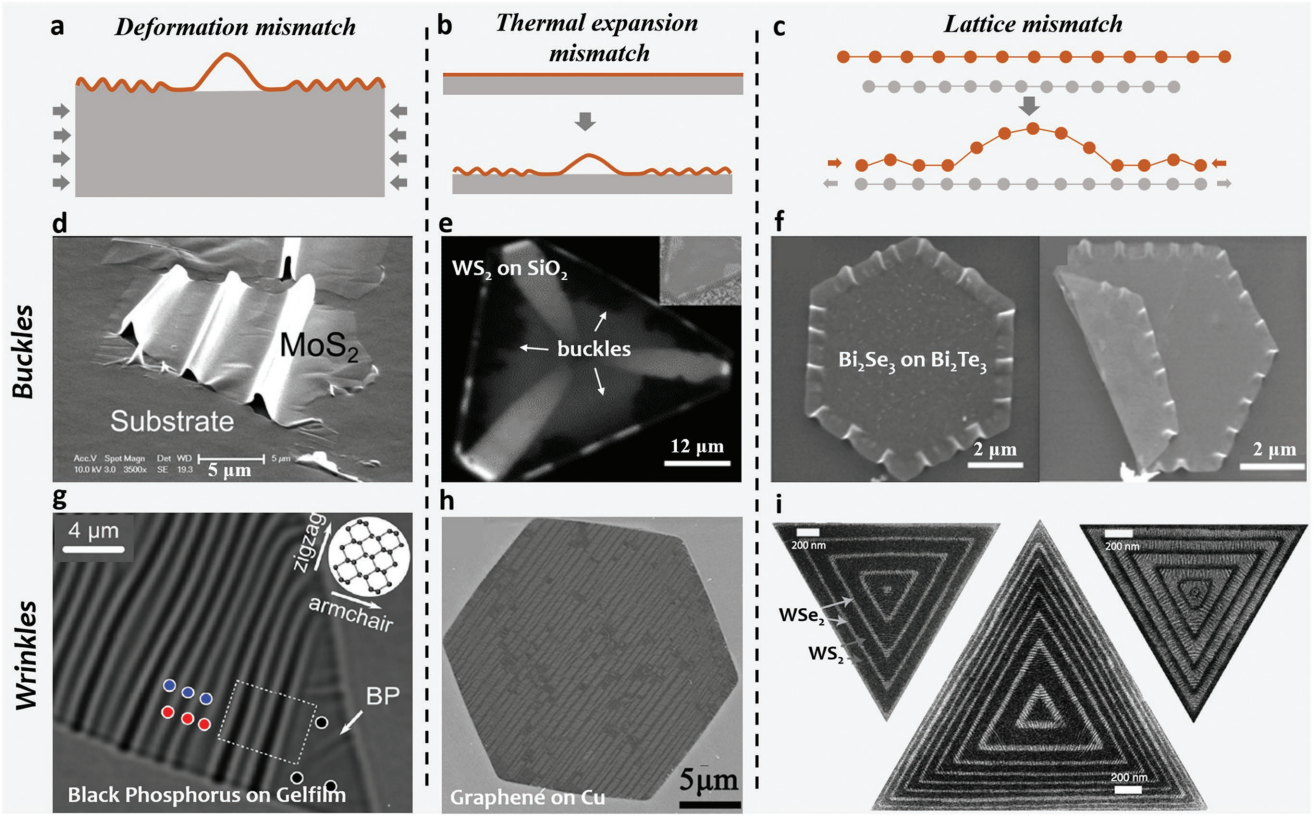

Figure 2. Out-of-plane mode: wrinkles and buckles. a–c) Scheme of buckles and wrinkles of 2D materials caused by compressing or prestretching a) the substrate, b) thermal-expansion mismatch, and c) lattice mismatch. d) Scanning electron microscopy (SEM) image of a buckled MoS_2 flake on an elastomeric substrate. d) Reproduced with permission.[46] Copyright 2013, American Chemical Society. e) PL intensity mapping image for a quasi-triangle monolayer WS_2 with edge buckle delamination. Reproduced with permission.[44] Copyright 2017, American Chemical Society. f) Tilted-view SEM image shows three buckles at each edge of the Bi_2Se_3/Bi_2Te_3 heterojunction. Reproduced with permission.[47] Copyright 2018, American Chemical Society. g) Optical image of a wrinkled 10 nm thick black phosphorus flake. The inset shows a sketch of the crystal lattice orientation. Reproduced with permission.[49] Copyright 2016, American Chemical Society. h) SEM image of a wrinkled, hexagonal graphene flake on copper. Reproduced with permission.[48] Copyright 2013, AIP Publishing. i) SEM images of three monolayer WS_2/WSe_2 superlattices. Reproduced with permission.[22] Copyright 2018, AAAS.

its applications in the hydrogen evolution reaction and band-gap engineering.[64–66] Notably, Choi et al. reported a three-step graphene integration technique to achieve a variety of 3D graphene patterns as partially shown in Figure 4c (elongated pyramids, rectangular pillars, and inverse pyramids).[68]

4. Mechanical Characterizations of the 2D Material–Substrate Interface

In the nanoscale regime, the vdW interactions between a 2D material and its substrate can have a strong influence on the mechanical behavior of 2D materials.[34,69] Consequently, the strain-coupled performance of 2D materials relies heavily on the mechanical behavior and properties of 2D-material-based vdW interfaces. For example, in the in-plane deformation mode, the strain in 2D materials is typically transferred from the substrate by the interfacial shear.[33,34,70,71] The maximal applicable strain to the 2D material hinges on the critical shear stress the vdW interface can undergo.[72–75] In the out-of-plane deformation mode, the 2D material–substrate adhesion (also called interfacial toughness) is one of the crucial parameters that dominate the wrinkling/buckling behavior,[41,42,76] determine the strain in bubbles and tents,[51–53,77–79] and predict the conformability between the thin membrane and the patterned substrate.[80] Such facts have motivated a lot of theoretical and experimental efforts into elucidating how these atomically thin 2D materials interact with their substrate. In the following, we focus on recent advances in experimental characterizations of interfacial shear and adhesion of 2D material–substrate interfaces. These results aim to provide a thorough understanding of the mechanical response of 2D material interfaces to both in-plane and out-of-plane deformations and ultimately offer direct guidelines for the optimal design of the strain engineering of 2D materials. The readers are also referred to detailed reviews on 2D material interfaces from different perspectives, such as of nanocomposites, tribology, and so on.[81–85]

4.1. Interfacial Shear

4.1.1. 2D Materials on a Substrate: Shear-Lag-Type Interfaces

Initially motivated by its importance in the field of nanocomposites, studies on the interfacial shear between graphene and

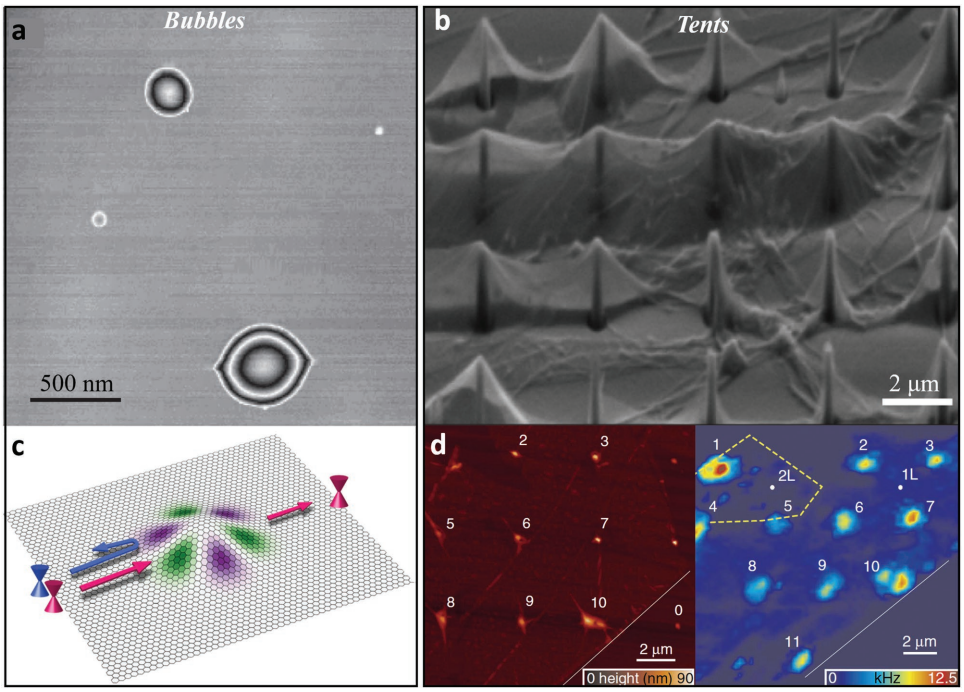

Figure 3. Out-of-plane mode: bubbles and tents. a) AFM image of graphene bubbles. Reproduced with permission.[52] Copyright 2016, Nature Publishing Group. b) SEM image of graphene tents formed by depositing onto a SiO_2 nanopillar array. Reproduced with permission.[62] Copyright 2014, American Chemical Society. c) An incoming incoming electron wave containing both *K* and *K′* valleys incident on a nanobubble experiences the associated pseudomagnetic field indicated by the color map. Reproduced with permission.[57] Copyright 2016, American Physical Society. d) AFM image (right panel) and corresponding peak PL signal map of the nanopillar-poked WSe_2 tent. Reproduced with permission.[59] Copyright 2017, Nature Publishing Group.

the substrate are now well established.[83,86,87] In this context, graphene is typically placed on a polymeric substrate such that one can stretch/compress the substrate and transfer such strain to the graphene sheet by interfacial shear (**Figure 5**a,b).[70,75,88] The distribution of the transferred strain in the whole graphene sheet can be further mapped by in situ monitoring the shift

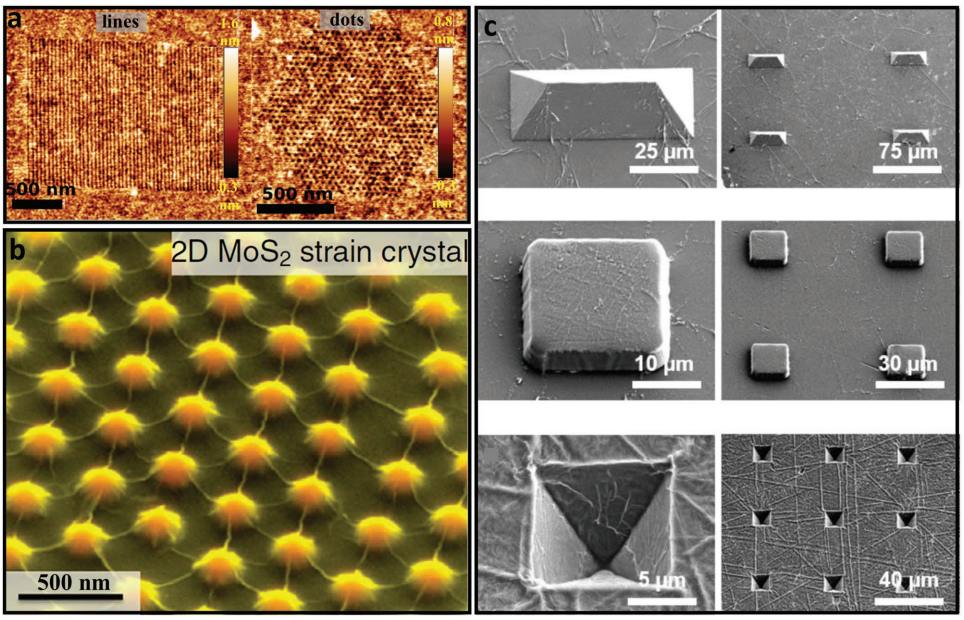

Figure 4. Out-of-plane mode: conformable patterns. a) AFM images of an indentation pattern of lines and dots. Reproduced with permission.[67] Copyright 2017, Nature Publishing Group. b) SEM image of strained MoS_2 on the nanocone substrate. Reproduced with permission.[66] Copyright 2015, Nature Publishing Group. c) SEM images of graphene conforming onto patterned substrates: elongated pyramids, rectangular pillars, and inverse pyramids. Reproduced with permission.[68] Copyright 2015, American Chemical Society.

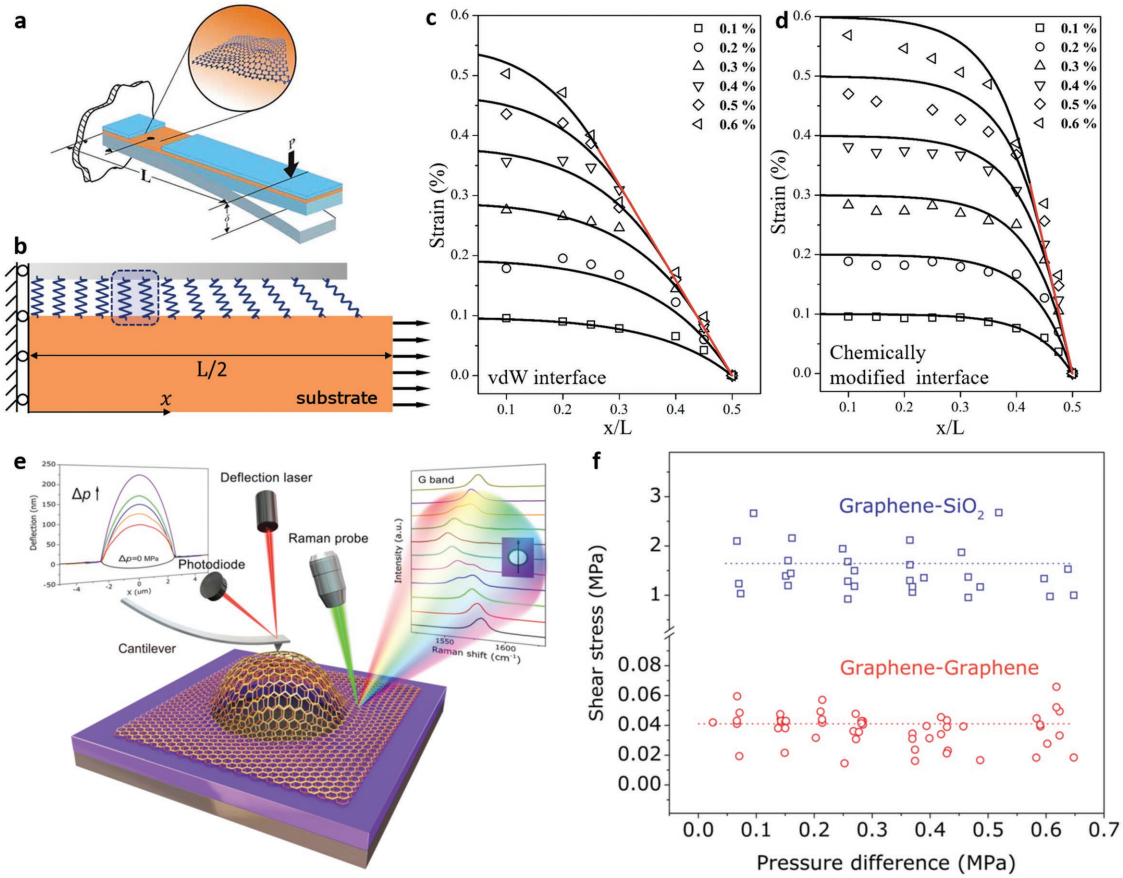

Figure 5. In-plane interfacial behaviors. a) Schematic diagram of applying tension to a monolayer graphene flake by a cantilever beam. Reproduced with permission.[70] Copyright 2009, Wiley-VCH. b) Simplified modeling in experiments: uniaxial stretch of the graphene/substrate system. c,d) Strain distribution along the tensile direction of monolayer graphene sheets on the substrate. The symbols represent experimentally measured data; solid lines are the analytical solution of nonlinear model for the vdW interface (c) and the hydrogen-bonded interface (d). b–d) Reproduced with permission.[75] Copyright 2016, Elsevier. e) Schematic diagram of a bilayer graphene bulging device and characterizations. The left inset shows profiles of a graphene bubble with increasing pressures. The right inset shows Raman spectra of a graphene G band stacked vertically in the direction of a line scan. f) Measured shear stresses for graphene–SiO_2 and graphene–graphene interfaces. The dashed lines correspond to the average values of 1.64 and 0.04 MPa. e–g) Reproduced with permission.[73] Copyright 2017, American Physical Society.

of Raman 2D or/and G peaks, leading to a quantitative understanding of interfacial shear properties.[83,86] Such a technique can also be applied to other 2D materials for the evaluation of their interfacial shear properties by the observation of the Raman shift of their characteristic bands when the supporting substrate is under strain.[87,89]

From the graphene/substrate systems, it is found that when the applied strain to the substrate is relatively small (e.g., <0.3% in Figure 5c), the distribution of transferred strain to graphene can be predicted by the classical shear-lag analysis. Strain builds up from the edges and approaches a peak at the center of graphene. Moreover, this peak strain is equal to the strain of the substrate when the interface interaction is strong, or the size of the graphene flake (L) is large. Quantitatively, the strain is fully transferred from the substrate to the center of graphene when $\beta L \gtrsim 10$, where $\beta L \left(= \sqrt{\frac{k}{E_{2D}}}\right)$ is an experimental fitting parameter comparing the shear stiffness of interface (k) to the 2D stiffness of graphene (E_{2D}). In fact, β is commonly treated as an effective measure of the interfacial stress transfer efficiency. As the applied strain increases, the strain distribution in graphene becomes almost linear near the edges (the red line in Figure 5c), an indicator of interfacial sliding with a constant shear stress at the interface. This constant stress, called interfacial shear strength (τ_c), can be determined from the linear slope, typically in the order of 1 MPa.[33,34,72,74,90]

The sliding-coupled shear-lag behaviors of graphene/substrate interfaces may extend for more general 2D material/amorphous substrate interfaces.[89,91] This experimental understanding provides many important implications for the strain engineering applications of 2D materials through in-plane deformation modes. Particularly, the unique sliding behavior of 2D material vdW interfaces defines the maximal strain the interface can transfer to 2D materials, which is $\frac{\tau_c L}{2E_{2D}}$. The large stiffness of 2D materials and the relatively weak interfacial shear strength can explain the limited strain (typically <4%) in 2D materials achieved by the in-plane deformation mode. Alternatively, this simple formulation highlights strategies to maximize the interface-transferred strain, such as by selecting

2D materials with large lateral size and by physically or chemically reinforcing the interfacial shear strength.[92] For example, Wang et al. and Dai and co-workers recently found that the interfacial shear strength of the hydrogen-bonded graphene/poly(methyl methacrylate) interface was calculated to be up to four times higher than that of pristine vdW interface as indicated by the increased slope of the red lines in Figure 5c,d.[74,90]

4.1.2. 2D Materials Subject to a Periodic Potential

Due to the production process or the operational requirements of 2D-material-based devices, 2D materials are frequently subject to periodic potentials, such as 2D materials on Ru, 2D material multilayers, and heterostructures.[17,20,22] In these cases, the shear deformation of the interfaces formed by two atomically smooth surfaces is critical for the overall functional performance, durability, and even fabrication of those devices.[73] A representative example is the epitaxial strain in CVD-grown 2D materials, which is much lower than theoretical expectations due to the relatively weak shear resistance between the 2D material and the underlying crystalline substrate.[17] Also, many exciting new physics in 2D material bilayers and heterostructures have been recently found to couple with the interlayer shear deformations, e.g., a simple mechanical twist.[93] However, experimental characterization of how the 2D material layer shears on a crystalline substrate or another 2D material layer is particularly challenging.

Wang et al. reported measurements of the interlayer shear stress in bilayer graphene based on pressurized microscale bubble loading devices (Figure 5e).[73] It was found that an interlayer shear zone outside the bubble edge could continuously propagate in a controlled manner and an interlayer shear stress of 40 kPa was extracted based on a membrane analysis for bilayer graphene bubbles. Comparatively, a much higher interfacial shear stress of 1.64 MPa was determined for monolayer graphene on a silicon oxide substrate (Figure 5f). However, these values were derived from Raman spectroscopy measurements with a spatial resolution of ≈1 μm and thus can be treated as spatially averaged interfacial shear properties of bilayer graphene. Recently, rich interfacial behaviors were observed from 2D material bilayers and heterostructures with characteristic length scales of a few nanometers.[24,25,94] For example, the interface in graphene bilayer and graphene–hBN heterostructure may rotate itself and cause strain in the 2D material lattice, driven by the vdW interaction.[24,94] Overall, research about 2D material multilayers and heterostructures is still considered to be in its beginnings (as illustrated later).[85,95]

4.2. Interfacial Adhesion

Extensive studies on macroscopic film/substrate systems have shown the essential role of interfacial adhesion in their collective mechanical behaviors.[42,96] Notably, many interesting out-of-plane deformation characteristics were observed and explained by comparing the elastic energy of the film with the interfacial adhesion.[76,77] For example, in a buckle with small amplitudes, the balance between adhesion (which favors large areas of contact) and bending energy (which is minimized for the buckle of large widths) dictates a constant curvature of the buckle crest: $d/\lambda^2 \sim \sqrt{\Delta\gamma/B}$.[76,97] d and λ are the width and height of the buckle, d/λ^2 represents the crest curvature, $\Delta\gamma$ is the interfacial adhesion, and B is the bending rigidity of the film. Similarly, in a bubble or tent (also called circular blister), the bending energy is negligible, while competition between the stretching energy of the film and the adhesion leads to a constant aspect ratio: $h/a \sim (\Delta\gamma/Et)^{1/4}$.[77] h and a are the height and the radius of the blister, E is the Young's modulus of the film, and t is the film thickness. Interestingly, these simple scaling relations, observed in bulk systems, are also true for the 2D material/substrate system. Examples include the constant crest curvatures of buckles formed by MoS_2 on silicone,[98] MoS_2 on poly(dimethylsiloxane), as well as the constant aspect ratios of bubbles (**Figure 6**a,b) formed by graphene on hBN, hBN on hBN, MoS_2 on hBN, MoS_2 on MoS_2, and many more.[52,78]

A straightforward output of those out-of-plane features in 2D material/substrate systems is to estimate the adhesion between the 2D material and its substrate. Graphene tents supported by nanoparticles have been made, and their aspect ratios have been utilized to measure the adhesion between graphene and its silicon substrate.[99] Recently, Deng et al. demonstrated the use of the crest curvature in a wrinkled MoS_2 to determine the adhesion energy between MoS_2 and its substrates.[98] More recently, Sanchez et al. developed a theoretical framework for estimating the work of adhesion of various 2D material interfaces using the experimentally measured aspect ratios of 2D-material bubbles (Figure 6c).[78] Moreover, as bubbles are almost inevitable when transferring 2D materials to a substrate in 2D material devices, a comprehensive adhesion map for various 2D interfaces may be constructed by "reading" bubble profiles (Figure 6c).[51–53,56] Knowing the interfacial adhesion of the 2D material to its substrate will be particularly convenient for the design of strain engineering devices of 2D materials through out-of-plane deformation modes. As above discussed, many features, such as the curvature of a buckle and the aspect ratio of a bubble or a tent can be predicted by comparing the elastic properties of 2D materials to the adhesion, and the associated in-plane strain is directly related to these features according to classical thin-plate theories.[9,46] Also, many behaviors, such as the onset of buckle delamination, wrinkle-to-buckle transition, conformability of the 2D material to a patterned substrate, and so on, may be deterministically designed, before actually fabricating these out-of-plane deformed devices.[39]

5. Applications, Challenges, and Opportunities

The strain engineering in silicon-based semiconductors has shown gigantic commercial success already, where a few percent of mechanical strain can achieve dramatic acceleration in carrier mobility by up to a few hundred percent. Extensive efforts are moving the strain engineering technology forward from silicon to 2D materials, which are intrinsically deformable. Extensive demonstrations have highlighted the essential role of mechanical strains in tuning the band

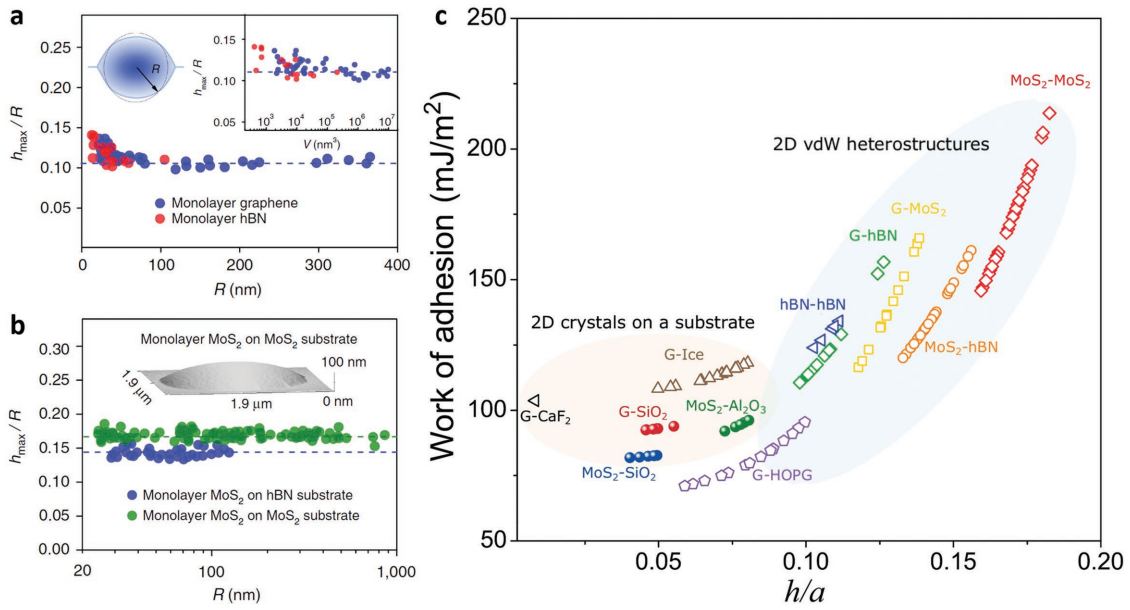

Figure 6. Interface adhesion. a) Aspect ratios as a function of the base radius for graphene (blue symbols) and monolayer hBN on bulk hBN (red symbols). Right inset: Aspect ratio of the bubbles as a function of their volume. b) Aspect ratio of MoS_2 bubbles on hBN and MoS_2 substrates. Inset: AFM image of a typical MoS_2 bubble. a,b) Reproduced with permission.[52] Copyright 2016, Nature Publishing Group. c) Work of adhesion values for various 2D material interfaces estimated according to blister profiles, including many interfaces found in 2D heterostructures. Reproduced with permission.[78] Copyright 2018, National Academy of Sciences.

structure of 2D materials. For example, asymmetrically distributed strain distributions can effectively open the band gap of semimetallic graphene sheets.[30,100] Transitions from direct to indirect band gap or from semiconductor to metal have further been reported by stretching TMDs.[36,101] For low-symmetry 2D materials such as black phosphorus, ReS_2, and so on, the band-gap response to mechanical strain becomes particularly sensitive to the loading direction.[49,102,103] More broadly, many fundamentals of 2D materials, including mechanical, optical, thermal, piezo/flexoelectrical, electromagnetic, and even catalytic, can be tuned and even substantially changed by straining their lattices, which are creating new physics and new applications. The readers are referred to comprehensive reviews for exciting details.[6,14,84,103,104] We conclude by discussing the current challenges limiting the development of the strain engineering of 2D materials, along with possible opportunities for future research as follows.

5.1. Synthesizing 2D Materials Capable of Surviving Large Strain

The family of 2D materials is becoming increasingly extended. Their applications, especially for strain-engineering purposes, implicitly depend on the mechanical properties for structural reliability and functional performances.[6] Most of these atomically thin layers are theoretically predicted to offer much larger strain limit compared to their bulk counterparts. Some of them, such as graphene and black phosphorus, have manifested their deformability (>10%) in nanoindentation tests.[82] However, microcracks might appear in 2D material/substrate devices at even 1% strain level, which have been frequently attributed to defects in the 2D lattice and brittleness of 2D materials.[12,105] In general, the emergence of defects in 2D materials, such as dopings, vacancies, and grain boundaries, might be inevitable either because of the fabrication process for mass production or because of functional requirements by which 2D material devices operate. Familiar examples are boron/nitrogen-doped graphene for band-gap opening and strained MoS_2 with S-vacancies for enhanced catalytic activity.[64,106] Therefore, it is still an open question to design 2D material from the atomic level for diverse functionalities without loss in (or even with enhanced) deformability.[107]

5.2. Applying Strain Magnitude and Distribution

Though various types of in-plane and out-of-plane modes have been proposed to deform 2D materials, both the strain magnitude and distribution are far from arbitrarily controlled. The bending-dominated modes (e.g., wrinkles and buckles) typically produce limited strain magnitude and periodic distributions.[46,49] By stretching-dominated modes (e.g., in-plane modes and bubbles), the effect of strain on the electronic properties of 2D materials was only reported based on strain levels of less than 6%.[89] Interesting physical and chemical phenomena emerging at large strain level or specific strain state shall be further experimentally investigated. Examples include the structural phase transition of MX_2 (likely appearing at large biaxial strain),[19,108] the uniform pseudomagnetic field in graphene (resulting from the uniform strain gradient),[109] the unique flexoelectricity in 2D materials (favoring maximal strain gradient),[6] and so on. In addition, although molecular simulations have demonstrated interesting wrinkling patterns associated with shear, realizing shear deformations in 2D materials

is still experimentally elusive, which may present an alternative and useful deformation mode for the strain engineering of 2D materials.[110]

5.3. Characterizing the vdW Interfaces

We may claim that in these in-plane and out-of-plane deformation modes summarized above, both strain magnitude and strain distribution can be estimated by understanding the associated interface. However, the rich interfacial behavior when 2D materials sit on a periodic potential (especially 2D materials on 2D materials—multilayers and heterostructures) is not completely clear so far. Recent observations of time- and temperature-dependent behaviors in 2D multilayers and heterostructures, such as self-folding, self-tearing, self-cleaning, and self-rotating, have highlighted the importance of mechanics within these ever-thin interfaces.[23,111] Unconventional superconductivity in so-called magic-angle graphene has further excited studies of new physics in slightly twisted 2D multilayers and heterostructures.[93] In these systems, the interface energy strongly couples the strain energy of the 2D material, leading to nanometer-sized hexagonal domains termed Moiré patterns.[85,94] The overall electronic and optoelectronic properties may hinge tightly on both the global strain in the layered structures (applied by the strain engineering techniques) and the local energy competition in the Moiré patterns (affected by the lattice mismatch, the twisting angle, and the type of materials) in a complex manner.[112] Such facts also call for both experimental and theoretical efforts to address this outstanding issue.

6. Conclusion

We have focused mainly on recent experimental achievements of in-plane and out-of-plane deformations in 2D materials and experimental characterization of the crucial role of 2D material–substrate interfaces in governing these deformations. Both the fundamental physics and exciting applications may emerge by taking advantage of deterministic control of the deformation and strain of 2D materials. We have also discussed the current challenges and potential opportunities in this interdisciplinary field for possible future research regarding physics, material sciences, and mechanics. However, only time will tell if 2D materials can be exploited as next-generation semiconductors in a scaled-up, reliable, cost-effective way, and if the strain engineering can achieve significant success from 2D materials as it did from silicon.

Acknowledgements

This project was jointly supported by the National Natural Science Foundation of China (Grant Nos. 21474023 and 11832010) and the National Key Basic Research Program of China (Grant Nos. 2013CB934203 and 2012CB937503).

Conflict of Interest

The authors declare no conflict of interest.

Keywords

2D materials, adhesion, interface, nanomechanics, strain engineering

Received: August 19, 2018
Revised: October 4, 2018
Published online:

[1] R. Mas-Balleste, C. Gomez-Navarro, J. Gomez-Herrero, F. Zamora, *Nanoscale* **2011**, *3*, 20.
[2] K. S. Novoselov, A. Mishchenko, A. Carvalho, A. H. Castro Neto, *Science* **2016**, *353*, aac9439.
[3] a) G. G. Naumis, S. Barraza-Lopez, M. Oliva-Leyva, H. Terrones, *Rep. Prog. Phys.* **2017**, *80*, 096501; b) R. Roldán, A. Castellanos-Gomez, E. Cappelluti, F. Guinea, *J. Phys.: Condens. Matter* **2015**, *27*, 313201; c) F. Guinea, M. Katsnelson, A. Geim, *Nat. Phys.* **2010**, *6*, 30.
[4] J. Li, Z. Shan, E. Ma, *MRS Bull.* **2014**, *39*, 108.
[5] C. Lee, X. Wei, J. W. Kysar, J. Hone, *Science* **2008**, *321*, 385.
[6] D. Akinwande, C. J. Brennan, J. S. Bunch, P. Egberts, J. R. Felts, H. Gao, R. Huang, J.-S. Kim, T. Li, Y. Li, K. M. Liechti, N. Lu, H. S. Park, E. J. Reed, P. Wang, B. I. Yakobson, T. Zhang, Y.-W. Zhang, Y. Zhou, Y. Zhu, *Extreme Mech. Lett.* **2017**, *13*, 42.
[7] a) D.-B. Zhang, E. Akatyeva, T. Dumitrică, *Phys. Rev. Lett.* **2011**, *106*, 255503; b) A. Castellanos-Gomez, M. Poot, G. A. Steele, H. S. van der Zant, N. Agraït, G. Rubio-Bollinger, *Adv. Mater.* **2012**, *24*, 772.
[8] F. De Juan, A. Cortijo, M. A. Vozmediano, A. Cano, *Nat. Phys.* **2011**, *7*, 810.
[9] J. Feng, X. Qian, C.-W. Huang, J. Li, *Nat. Photonics* **2012**, *6*, 866.
[10] N. N. Klimov, S. Jung, S. Zhu, T. Li, C. A. Wright, S. D. Solares, D. B. Newell, N. B. Zhitenev, J. A. Stroscio, *Science* **2012**, *336*, 1557.
[11] M. Goldsche, J. Sonntag, T. Khodkov, G. J. Verbiest, S. Reichardt, C. Neumann, T. Ouaj, N. von den Driesch, D. Buca, C. Stampfer, *Nano Lett.* **2018**, *18*, 1707.
[12] D. Akinwande, N. Petrone, J. Hone, *Nat. Commun.* **2014**, *5*, 5678.
[13] a) X. Xu, C. Liu, Z. Sun, T. Cao, Z. Zhang, E. Wang, Z. Liu, K. Liu, *Chem. Soc. Rev.* **2018**, *47*, 3059; b) G. Zhao, X. Li, M. Huang, Z. Zhen, Y. Zhong, Q. Chen, X. Zhao, Y. He, R. Hu, T. Yang, *Chem. Soc. Rev.* **2017**, *46*, 4417; c) Y. Liu, X. Duan, Y. Huang, X. Duan, *Chem. Soc. Rev.* **2018**, *47*, 6388; d) F. Wang, Z. Wang, L. Yin, R. Cheng, J. Wang, Y. Wen, T. A. Shifa, F. Wang, Y. Zhang, X. Zhan, J. He, *Chem. Soc. Rev.* **2018**, *47*, 6296; e) H. Zhang, M. Chhowalla, Z. Liu, *Chem. Soc. Rev.* **2018**, *47*, 3015; f) X. Zhang, Q.-H. Tan, J.-B. Wu, W. Shi, P.-H. Tan, *Nanoscale* **2016**, *8*, 6435; g) F. Ceballos, H. Zhao, *Adv. Funct. Mater.* **2017**, *27*, 1604509; h) X. Lu, X. Luo, J. Zhang, S. Y. Quek, Q. Xiong, *Nano Res.* **2016**, *9*, 3559.
[14] S. Deng, A. V. Sumant, V. Berry, *Nano Today*, **2018**, *22*, 14.
[15] J. A. Del Alamo, *Nature* **2011**, *479*, 317.
[16] L. B. Freund, S. Suresh, *Thin Film Materials: Stress, Defect Formation and Surface Evolution*, Cambridge University Press, New York **2004**.
[17] G. H. Ahn, M. Amani, H. Rasool, D.-H. Lien, J. P. Mastandrea, J. W. Ager III, M. Dubey, D. C. Chrzan, A. M. Minor, A. Javey, *Nat. Commun.* **2017**, *8*, 608.
[18] a) M. Amani, M. L. Chin, A. L. Mazzoni, R. A. Burke, S. Najmaei, P. M. Ajayan, J. Lou, M. Dubey, *Appl. Phys. Lett.* **2014**, *104*, 203506; b) Z. Liu, M. Amani, S. Najmaei, Q. Xu, X. Zou, W. Zhou, T. Yu, C. Qiu, A. G. Birdwell, F. J. Crowne, *Nat. Commun.* **2014**, *5*, 5246.
[19] K.-A. N. Duerloo, Y. Li, E. J. Reed, *Nat. Commun.* **2014**, *5*, 4214.
[20] M.-Y. Li, Y. Shi, C.-C. Cheng, L.-S. Lu, Y.-C. Lin, H.-L. Tang, M.-L. Tsai, C.-W. Chu, K.-H. Wei, J.-H. He, *Science* **2015**, *349*, 524.

[21] a) Y. Han, K. X. Nguyen, M. Cao, P. D. Cueva, S. Xie, M. W. Tate, P. Purohit, S. M. Gruner, J. Park, D. A. Muller, *Nano Lett.* **2018**, *18*, 3746; b) C. Zhang, M.-Y. Li, J. Tersoff, Y. Han, Y. Su, L.-J. Li, D. A. Muller, C.-K. Shih, *Nat. Nanotechnol.* **2018**, *13*, 152.
[22] S. Xie, L. Tu, Y. Han, L. Huang, K. Kang, K. U. Lao, P. Poddar, C. Park, D. A. Muller, R. A. DiStasio, *Science* **2018**, *359*, 1131.
[23] A. K. Geim, I. V. Grigorieva, *Nature* **2013**, *499*, 419.
[24] C. Woods, F. Withers, M. Zhu, Y. Cao, G. Yu, A. Kozikov, M. B. Shalom, S. Morozov, M. Van Wijk, A. Fasolino, *Nat. Commun.* **2016**, *7*, 10800.
[25] C. Woods, L. Britnell, A. Eckmann, R. Ma, J. Lu, H. Guo, X. Lin, G. Yu, Y. Cao, R. Gorbachev, *Nat. Phys.* **2014**, *10*, 451.
[26] S.-W. Wang, H. Medina, K.-B. Hong, C.-C. Wu, Y. Qu, A. Manikandan, T.-Y. Su, P.-T. Lee, Z.-Q. Huang, Z. Wang, *ACS Nano* **2017**, *11*, 8768.
[27] G. Plechinger, A. Castellanos-Gomez, M. Buscema, H. S. van der Zant, G. A. Steele, A. Kuc, T. Heine, C. Schüller, T. Korn, *2D Mater.* **2015**, *2*, 015006.
[28] G. Wang, L. Liu, Z. Dai, Q. Liu, H. Miao, Z. Zhang, *Carbon* **2015**, *86*, 69.
[29] T. Mohiuddin, A. Lombardo, R. Nair, A. Bonetti, G. Savini, R. Jalil, N. Bonini, D. Basko, C. Galiotis, N. Marzari, *Phys. Rev. B* **2009**, *79*, 205433.
[30] Z. H. Ni, T. Yu, Y. H. Lu, Y. Y. Wang, Y. P. Feng, Z. X. Shen, *ACS Nano* **2008**, *2*, 2301.
[31] a) W. Wu, J. Wang, P. Ercius, N. C. Wright, D. M. Leppert-Simenauer, R. A. Burke, M. Dubey, A. M. Dogare, M. T. Pettes, *Nano Lett.* **2018**, *18*, 2351; b) K. He, C. Poole, K. F. Mak, J. Shan, *Nano Lett.* **2013**, *13*, 2931.
[32] S. Yang, C. Wang, H. Sahin, H. Chen, Y. Li, S.-S. Li, A. Suslu, F. M. Peeters, Q. Liu, J. Li, *Nano Lett.* **2015**, *15*, 1660.
[33] T. Jiang, R. Huang, Y. Zhu, *Adv. Funct. Mater.* **2014**, *24*, 396.
[34] a) L. Gong, I. A. Kinloch, R. J. Young, I. Riaz, R. Jalil, K. S. Novoselov, *Adv. Mater.* **2010**, *22*, 2694; b) Z. Dai, Y. Wang, L. Liu, X. Liu, P. Tan, Z. Xu, J. Kuang, Q. Liu, J. Lou, Z. Zhang, *Adv. Funct. Mater.* **2016**, *26*, 7003.
[35] A. P. A. Raju, A. Lewis, B. Derby, R. J. Young, I. A. Kinloch, R. Zan, K. S. Novoselov, *Adv. Funct. Mater.* **2014**, *24*, 2865.
[36] R. Yang, J. Lee, S. Ghosh, H. Tang, R. M. Sankaran, C. A. Zorman, P. X.-L. Feng, *Nano Lett.* **2017**, *17*, 4568.
[37] J. Liang, J. Zhang, Z. Li, H. Hong, J. Wang, Z. Zhang, X. Zhou, R. Qiao, J. Xu, P. Gao, *Nano Lett.* **2017**, *17*, 7539.
[38] M. C. Wang, J. Leem, P. Kang, J. Choi, P. Knapp, K. Yong, S. Nam, *2D Mater.* **2017**, *4*, 022002.
[39] S. Deng, V. Berry, *Mater. Today* **2016**, *19*, 197.
[40] a) H. Jiang, D.-Y. Khang, J. Song, Y. Sun, Y. Huang, J. A. Rogers, *Proc. Natl. Acad. Sci. USA* **2007**, *104*, 15607; b) A. Kushima, X. Qian, P. Zhao, S. Zhang, J. Li, *Nano Lett.* **2015**, *15*, 1302.
[41] K. Pan, Y. Ni, L. He, R. Huang, *Int. J. Solids Struct.* **2014**, *51*, 3715.
[42] Q. Zhang, J. Yin, *J. Mech. Phys. Solids* **2018**, *118*, 40.
[43] P. Y. Chen, J. Sodhi, Y. Qiu, T. M. Valentin, R. S. Steinberg, Z. Wang, R. H. Hurt, I. Y. Wong, *Adv. Mater.* **2016**, *28*, 3564.
[44] T. H. Ly, S. J. Yun, Q. H. Thi, J. Zhao, *ACS Nano* **2017**, *11*, 7534.
[45] H. Hattab, A. T. N'Diaye, D. Wall, C. Klein, G. Jnawali, J. Coraux, C. Busse, R. van Gastel, B. Poelsema, T. Michely, *Nano Lett.* **2012**, *12*, 678.
[46] A. Castellanos-Gomez, R. Roldán, E. Cappelluti, M. Buscema, F. Guinea, H. S. van der Zant, G. A. Steele, *Nano Lett.* **2013**, *13*, 5361.
[47] S. Lou, Y. Liu, F. Yang, S. Lin, R. Zhang, Y. Deng, M. Wang, K. B. Tom, F. Zhou, H. Ding, K. C. Bustillo, X. Wang, S. Yan, M. Scott, A. Minor, J. Yao, *Nano Lett.* **2018**, *18*, 1819.
[48] L. Meng, Y. Su, D. Geng, G. Yu, Y. Liu, R.-F. Dou, J.-C. Nie, L. He, *Appl. Phys. Lett.* **2013**, *103*, 251610.
[49] J. Quereda, P. San-Jose, V. Parente, L. Vaquero-Garzon, A. J. Molina-Mendoza, N. Agraït, G. Rubio-Bollinger, F. Guinea, R. Roldán, A. Castellanos-Gomez, *Nano Lett.* **2016**, *16*, 2931.
[50] C. J. Brennan, J. Nguyen, E. T. Yu, N. Lu, *Adv. Mater. Interfaces* **2015**, *2*, 1500176.
[51] H. Ghorbanfekr-Kalashami, K. S. Vasu, R. R. Nair, F. M. Peeters, M. Neek-Amal, *Nat. Commun.* **2017**, *8*, 15844.
[52] E. Khestanova, F. Guinea, L. Fumagalli, A. K. Geim, I. V. Grigorieva, *Nat. Commun.* **2016**, *7*, 12587.
[53] K. Vasu, E. Prestat, J. Abraham, J. Dix, R. Kashtiban, J. Beheshtian, J. Sloan, P. Carbone, M. Neek-Amal, S. Haigh, *Nat. Commun.* **2016**, *7*, 12168.
[54] a) H. Yoshida, V. Kaiser, B. Rotenberg, L. Bocquet, *Nat. Commun.* **2018**, *9*, 1496; b) G. Zamborlini, M. Imam, L. L. Patera, T. O. Menteş, N. a. Stojić, C. Africh, A. Sala, N. Binggeli, G. Comelli, A. Locatelli, *Nano Lett.* **2015**, *15*, 6162.
[55] A. Kretinin, Y. Cao, J. Tu, G. Yu, R. Jalil, K. Novoselov, S. Haigh, A. Gholinia, A. Mishchenko, M. Lozada, *Nano Lett.* **2014**, *14*, 3270.
[56] F. Pizzocchero, L. Gammelgaard, B. S. Jessen, J. M. Caridad, L. Wang, J. Hone, P. Boggild, T. J. Booth, *Nat. Commun.* **2016**, *7*, 11894.
[57] M. Settnes, S. R. Power, M. Brandbyge, A.-P. Jauho, *Phys. Rev. Lett.* **2016**, *117*, 276801.
[58] N. Levy, S. Burke, K. Meaker, M. Panlasigui, A. Zettl, F. Guinea, A. C. Neto, M. Crommie, *Science* **2010**, *329*, 544.
[59] A. Branny, S. Kumar, R. Proux, B. D. Gerardot, *Nat. Commun.* **2017**, *8*, 15053.
[60] Z. Chen, K. Leng, X. Zhao, S. Malkhandi, W. Tang, B. Tian, L. Dong, L. Zheng, M. Lin, B. S. Yeo, *Nat. Commun.* **2017**, *8*, 14548.
[61] Y. Jiang, J. Mao, J. Duan, X. Lai, K. Watanabe, T. Taniguchi, E. Y. Andrei, *Nano Lett.* **2017**, *17*, 2839.
[62] A. Reserbat-Plantey, D. Kalita, Z. Han, L. Ferlazzo, S. Autier-Laurent, K. Komatsu, C. Li, R. l. Weil, A. Ralko, L. T. Marty, *Nano Lett.* **2014**, *14*, 5044.
[63] a) Y. Zhang, M. Heiranian, B. Janicek, Z. Budrikis, S. Zapperi, P. Y. Huang, H. T. Johnson, N. R. Aluru, J. W. Lyding, N. Mason, *Nano Lett.* **2018**, *18*, 2098; b) B. G. Shin, G. H. Han, S. J. Yun, H. M. Oh, J. J. Bae, Y. J. Song, C. Y. Park, Y. H. Lee, *Adv. Mater.* **2016**, *28*, 9378.
[64] H. Li, C. Tsai, A. L. Koh, L. Cai, A. W. Contryman, A. H. Fragapane, J. Zhao, H. S. Han, H. C. Manoharan, F. Abild-Pedersen, *Nat. Mater.* **2016**, *15*, 48.
[65] H. Li, M. Du, M. J. Mleczko, A. L. Koh, Y. Nishi, E. Pop, A. J. Bard, X. Zheng, *J. Am. Chem. Soc.* **2016**, *138*, 5123.
[66] H. Li, A. W. Contryman, X. Qian, S. M. Ardakani, Y. Gong, X. Wang, J. M. Weisse, C. H. Lee, J. Zhao, P. M. Ajayan, *Nat. Commun.* **2015**, *6*, 7381.
[67] P. Nemes-Incze, G. Kukucska, J. Koltai, J. Kürti, C. Hwang, L. Tapasztó, L. P. Biró, *Sci. Rep.* **2017**, *7*, 3035.
[68] J. Choi, H. J. Kim, M. C. Wang, J. Leem, W. P. King, S. Nam, *Nano Lett.* **2015**, *15*, 4525.
[69] S. P. Koenig, N. G. Boddeti, M. L. Dunn, J. S. Bunch, *Nat. Nanotechnol.* **2011**, *6*, 543.
[70] G. Tsoukleri, J. Parthenios, K. Papagelis, R. Jalil, A. C. Ferrari, A. K. Geim, K. S. Novoselov, C. Galiotis, *Small* **2009**, *5*, 2397.
[71] a) Y. Liu, Z. Xu, Q. Zheng, *J. Mech. Phys. Solids* **2011**, *59*, 1613; b) A. L. Kitt, Z. Qi, S. Rémi, H. S. Park, A. K. Swan, B. B. Goldberg, *Nano Lett.* **2013**, *13*, 2605.
[72] G. Guo, Y. Zhu, *J. Appl. Mech.* **2015**, *82*, 031005.
[73] G. Wang, Z. Dai, Y. Wang, P. Tan, L. Liu, Z. Xu, Y. Wei, R. Huang, Z. Zhang, *Phys. Rev. Lett.* **2017**, *119*, 036101.
[74] G. Wang, E. Gao, Z. Dai, L. Liu, Z. Xu, Z. Zhang, *Compos. Sci. Technol.* **2017**, *149*, 220.

[75] Z. Dai, G. Wang, L. Liu, Y. Hou, Y. Wei, Z. Zhang, *Compos. Sci. Technol.* **2016**, *136*, 1.
[76] D. Vella, J. Bico, A. Boudaoud, B. Roman, P. M. Reis, *Proc. Natl. Acad. Sci. USA* **2009**, *106*, 10901.
[77] J. Chopin, D. Vella, A. Boudaoud, *Proc. R. Soc. London, Ser. A* **2008**, *464*, 2887.
[78] D. A. Sanchez, Z. Dai, P. Wang, A. Cantu-Chavez, C. J. Brennan, R. Huang, N. Lu, *Proc. Natl. Acad. Sci. USA* **2018**, *115*, 7884.
[79] a) K. Yue, W. Gao, R. Huang, K. M. Liechti, *J. Appl. Phys.* **2012**, *112*, 083512; b) P. Wang, W. Gao, Z. Cao, K. M. Liechti, R. Huang, *J. Appl. Mech.* **2013**, *80*, 040905.
[80] a) Z. Zhang, T. Li, *J. Appl. Phys.* **2011**, *110*, 083526; b) L. Wang, S. Qiao, S. K. Ameri, H. Jeong, N. Lu, *J. Appl. Mech.* **2017**, *84*, 111003; c) L. Wang, N. Lu, *J. Appl. Mech.* **2016**, *83*, 041007.
[81] a) H. D. Wagner, R. A. Vaia, *Mater. Today* **2004**, *7*, 38; b) Q. Li, M. Liu, Y. Zhang, Z. Liu, *Small* **2016**, *12*, 32.
[82] C. Androulidakis, K. Zhang, M. Robertson, S. H. Tawfick, *2D Mater.* **2018**, *5*, 032005.
[83] D. G. Papageorgiou, I. A. Kinloch, R. J. Young, *Prog. Mater. Sci.* **2017**, *90*, 75.
[84] J. C. Spear, B. W. Ewers, J. D. Batteas, *Nano Today* **2015**, *10*, 301.
[85] P. Pochet, B. C. McGuigan, J. Coraux, H. T. Johnson, *Appl. Mater. Today* **2017**, *9*, 240.
[86] R. J. Young, I. A. Kinloch, L. Gong, K. S. Novoselov, *Compos. Sci. Technol.* **2012**, *72*, 1459.
[87] Q. Zhang, Z. Chang, G. Xu, Z. Wang, Y. Zhang, Z. Q. Xu, S. Chen, Q. Bao, J. Z. Liu, Y. W. Mai, *Adv. Funct. Mater.* **2016**, *26*, 8707.
[88] Y. Wang, Y. Wang, C. Xu, X. Zhang, L. Mei, M. Wang, Y. Xia, P. Zhao, H. Wang, *Carbon* **2018**, *134*, 37.
[89] H. J. Conley, B. Wang, J. I. Ziegler, R. F. Haglund Jr., S. T. Pantelides, K. I. Bolotin, *Nano Lett.* **2013**, *13*, 3626.
[90] G. Wang, Z. Dai, L. Liu, H. Hu, Q. Dai, Z. Zhang, *ACS Appl. Mater. Interfaces* **2016**, *8*, 22554.
[91] M. S. Bronsgeest, N. Bendiab, S. Mathur, A. Kimouche, H. T. Johnson, J. Coraux, P. Pochet, *Nano Lett.* **2015**, *15*, 5098.
[92] a) G. Wang, X. Li, Y. Wang, Z. Zheng, Z. Dai, X. Qi, L. Liu, Z. Cheng, Z. Xu, P. Tan, *J. Phys. Chem. C* **2017**, *121*, 26034; b) C. Xu, T. Xue, W. Qiu, Y. Kang, *ACS Appl. Mater. Interfaces* **2016**, *8*, 27099.
[93] a) Y. Cao, V. Fatemi, S. Fang, K. Watanabe, T. Taniguchi, E. Kaxiras, P. Jarillo-Herrero, *Nature* **2018**, *556*, 43; b) Y. Cao, V. Fatemi, A. Demir, S. Fang, S. L. Tomarken, J. Y. Luo, J. D. Sanchez-Yamagishi, K. Watanabe, T. Taniguchi, E. Kaxiras, *Nature* **2018**, *556*, 80.
[94] K. Zhang, E. B. Tadmor, *J. Mech. Phys. Solids* **2018**, *112*, 225.
[95] a) O. Hod, M. Urbakh, D. Naveh, M. Bar-Sadan, A. Ismach, *Adv. Mater.* **2018**, *30*, 1706581; b) J. Li, T. Gao, J. Luo, *Adv. Sci.* **2018**, *5*, 1700616; c) H. Li, J. Wang, S. Gao, Q. Chen, L. Peng, K. Liu, X. Wei, *Adv. Mater.* **2017**, *29*, 1701474.
[96] R. Huang, *J. Mech. Phys. Solids* **2005**, *53*, 63.
[97] Y. Aoyanagi, J. Hure, J. Bico, B. Roman, *Soft Matter* **2010**, *6*, 5720.
[98] S. Deng, E. Gao, Z. Xu, V. Berry, *ACS Appl. Mater. Interfaces* **2017**, *9*, 7812.
[99] a) Z. Zong, C.-L. Chen, M. R. Dokmeci, K.-T. Wan, *J. Appl. Phys.* **2010**, *107*, 026104; b) X. Gao, X. Yu, B. Li, S. Fan, C. Li, *Adv. Mater. Interfaces* **2017**, *4*, 1601023.
[100] G. Gui, J. Li, J. Zhong, *Phys. Rev. B* **2008**, *78*, 075435.
[101] a) Y. Wang, C. Cong, C. Qiu, T. Yu, *Small* **2013**, *9*, 2857; b) P. Johari, V. B. Shenoy, *ACS Nano* **2012**, *6*, 5449.
[102] a) S. Tongay, H. Sahin, C. Ko, A. Luce, W. Fan, K. Liu, J. Zhou, Y.-S. Huang, C.-H. Ho, J. Yan, *Nat. Commun.* **2014**, *5*, 3252; b) C. Yang, J. Zhang, G. Wang, C. Zhang, *Phys. Rev. B* **2018**, *97*, 245408; c) B. Liao, H. Zhao, E. Najafi, X. Yan, H. Tian, J. Tice, A. J. Minnich, H. Wang, A. H. Zewail, *Nano Lett.* **2017**, *17*, 3675; d) B. Deng, V. Tran, Y. Xie, H. Jiang, C. Li, Q. Guo, X. Wang, H. Tian, S. J. Koester, H. Wang, *Nat. Commun.* **2017**, *8*, 14474.
[103] H. Tian, J. Tice, R. Fei, V. Tran, X. Yan, L. Yang, H. Wang, *Nano Today* **2016**, *11*, 763.
[104] B. Amorim, A. Cortijo, F. De Juan, A. Grushin, F. Guinea, A. Gutiérrez-Rubio, H. Ochoa, V. Parente, R. Roldán, P. San-Jose, *Phys. Rep.* **2016**, *617*, 1.
[105] a) P. Zhang, L. Ma, F. Fan, Z. Zeng, C. Peng, P. E. Loya, Z. Liu, Y. Gong, J. Zhang, X. Zhang, P. M. Ajayan, T. Zhu, J. Lou, *Nat. Commun.* **2014**, *5*, 3782; b) J.-H. Lee, D.-W. Jang, S.-G. Hong, B. C. Park, J.-H. Kim, H.-J. Jung, S.-B. Lee, *Carbon* **2017**, *118*, 475; c) S. R. Na, X. Wang, R. D. Piner, R. Huang, C. G. Willson, K. M. Liechti, *ACS Nano* **2016**, *10*, 9616.
[106] L. Panchakarla, K. Subrahmanyam, S. Saha, A. Govindaraj, H. Krishnamurthy, U. Waghmare, C. Rao, *Adv. Mater.* **2009**, *21*, 4726.
[107] a) E. F. Hacopian, Y. Yang, B. Ni, Y. Li, X. Li, Q. Chen, H. Guo, J. M. Tour, H. Gao, J. Lou, *ACS Nano* **2018**, *12*, 7901; b) T. Zhang, X. Li, H. Gao, *Int. J. Fract.* **2015**, *196*, 1.
[108] a) A. Apte, V. Kochat, P. Rajak, A. Krishnamoorthy, P. Manimunda, J. A. Hachtel, J. C. Idrobo, S. A. Syed Amanulla, P. Vashishta, A. Nakano, *ACS Nano* **2018**, *12*, 3468; b) S. Song, D. H. Keum, S. Cho, D. Perello, Y. Kim, Y. H. Lee, *Nano Lett.* **2016**, *16*, 188.
[109] a) Z. Qi, A. L. Kitt, H. S. Park, V. M. Pereira, D. K. Campbell, A. C. Neto, *Phys. Rev. B* **2014**, *90*, 125419; b) S. Zhu, Y. Huang, N. N. Klimov, D. B. Newell, N. B. Zhitenev, J. A. Stroscio, S. D. Solares, T. Li, *Phys. Rev. B* **2014**, *90*, 075426; c) S. Zhu, J. A. Stroscio, T. Li, *Phys. Rev. Lett.* **2015**, *115*, 245501.
[110] a) C. Wang, Y. Liu, L. Lan, H. Tan, *Nanoscale* **2013**, *5*, 4454; b) Z. Qin, M. Taylor, M. Hwang, K. Bertoldi, M. J. Buehler, *Nano Lett.* **2014**, *14*, 6520.
[111] a) D. Wang, G. Chen, C. Li, M. Cheng, W. Yang, S. Wu, G. Xie, J. Zhang, J. Zhao, X. Lu, *Phys. Rev. Lett.* **2016**, *116*, 126101; b) J. Annett, G. L. Cross, *Nature* **2016**, *535*, 271.
[112] a) L. Gao, X. Chen, Y. Ma, Y. Yan, T. Ma, Y. Su, L. Qiao, *Nanoscale* **2018**, *10*, 10576; b) L. Huder, A. Artaud, T. Le Quang, G. T. de Laissardiere, A. G. Jansen, G. Lapertot, C. Chapelier, V. T. Renard, *Phys. Rev. Lett.* **2018**, *120*, 156405; c) L. Jiang, S. Wang, Z. Shi, C. Jin, M. I. B. Utama, S. Zhao, Y.-R. Shen, H.-J. Gao, G. Zhang, F. Wang, *Nat. Nanotechnol.* **2018**, *13*, 204; d) M. L. Lin, Q. H. Tan, J. B. Wu, X. S. Chen, J. H. Wang, Y. H. Pan, X. Zhang, X. Cong, J. Zhang, W. Ji, P. A. Hu, K. H. Liu, P. H. Tan, *ACS Nano* **2018**, *12*, 8770; e) W. Ouyang, D. Mandelli, M. Urbakh, O. Hod, *Nano Lett.* **2018**, *18*, 6009; f) R. Ribeiro-Palau, C. J. Zhang, K. Watanabe, T. Taniguchi, J. Hone, C. R. Dean, *Science* **2018**, *361*, 690; g) P. Schweizer, C. Dolle, E. Spiecker, *Sci. Adv.* **2018**, *4*, eaat4712; h) A. Summerfield, A. Kozikov, T. S. Cheng, A. Davies, Y. J. Cho, A. N. Khlobystov, C. J. Mellor, C. T. Foxon, K. Watanabe, T. Taniguchi, L. Eaves, K. S. Novoselov, S. V. Novikov, P. H. Beton, *Nano Lett.* **2018**, *18*, 4241; i) M. Yankowitz, J. Jung, E. Laksono, N. Leconte, B. L. Chittari, K. Watanabe, T. Taniguchi, S. Adam, D. Graf, C. R. Dean, *Nature* **2018**, *557*, 404; j) W. Yao, E. Wang, C. Bao, Y. Zhang, K. Zhang, K. Bao, C. K. Chan, C. Chen, J. Avila, M. C. Asensio, *Proc. Natl. Acad. Sci. USA* **2018**, *115*, 6928; k) X. Zhao, Z. Ding, J. Chen, J. Dan, S. M. Poh, W. Fu, S. J. Pennycook, W. Zhou, K. P. Loh, *ACS Nano* **2018**, *12*, 1940.